Published in final edited form as:
Nucleosides Nucleotides Nucleic Acids. 2009 May ; 28(5): 352–378. doi:10.1080/15257770903044523.

Thiophosphate Analogs of c-di-GMP: Impact on Polymorphism

Jianwei Zhao, **Elizabeth Veliath**, **Seho Kim**, **Barbara L. Gaffney**, and **Roger A. Jones**
Department of Chemistry and Chemical Biology, Rutgers, The State University of New Jersey, Piscataway, New Jersey, 08854 USA

Jianwei Zhao: ; Elizabeth Veliath: ; Seho Kim: ; Barbara L. Gaffney: ; Roger A. Jones: r.jones@rutgers.edu

Abstract

Seven phosphorothioate analogs of c-di-GMP (all diastereomers of mono-, di-, and trithiophosphates) were prepared to assess the impact of the thioate substitutions on c-di-GMP polymorphism using 1D ^{1}H and ^{31}P NMR, along with 2D NOESY and DOSY, for both the Na^+ and K^+ salts. The K^+ salts display more extensive higher order complex formation than the Na^+ salts, resulting primarily in octamolecular complexes with K^+, but tetramolecular complexes with Na^+. Further, the presence of one or two [S_P] sulfurs specifically stabilizes anti complexes and/or destabilizes syn complexes, while the presence of two [S_P] sulfurs promotes extensive aggregation.

Keywords

c-di-GMP; thiophosphates; polymorphism; guanine quartets

INTRODUCTION

The bacterial signaling molecule, cyclic diguanosine monophosphate (c-di-GMP, Figure 1), is increasingly recognized as having widespread consequences for human health through its multiple roles.[1–4] Not only is c-di-GMP a major factor in the activation of bacterial biofilm formation and repression of motility, it also helps to regulate virulence. Further, although c-di-GMP is not a signaling molecule in Eukarya, it has been shown to be an immunostimulatory agent that can trigger the innate immune response in mice.[5,6] Yet the mechanisms for how c-di-GMP functions remain unclear. Studies using a series of analogs of c-di-GMP[7] should facilitate elucidation of its modes of action, and would also allow evaluation of their potential use in the design of new therapeutic agents.

We have recently reported a new synthetic procedure for c-di-GMP,8 as well as a description of its concentration and metal dependent polymorphism.[9] In addition to a self-intercalated bimolecular structure, the molecule can adopt four different but related higher order guanine quartet structures, all in slow equilibrium. We also demonstrated that the analog in which one guanine residue is replaced with hypoxanthine (c-GMP-IMP) does not adopt these higher order complexes, presumably because the absence of even one guanine amino group precludes quartet formation.[9]

We now present results for a new family of analogs of c-di-GMP: a series of seven phosphorothioate derivatives that includes all diastereomers of mono-, di-, and trithiophosphates. The [R_P] and [S_P] monothiophosphates of c-di-GMP had been synthesized

Correspondence to: Roger A. Jones, r.jones@rutgers.edu.
In honor of and in celebration of Morris J. Robins' 70th birthday

some years ago by a triester method as part of a study of the regulatory system of bacterial cellulose synthesis.[10] Both diastereomers proved to be effective activators of cellulose synthase,[10] while showing resistance to hydrolysis by a specific phosphodiesterase. A more recent synthesis of these monothiophosphates of c-di-GMP has been reported that used an initial amidite coupling, followed by a triester cyclization, without separation of the diastereomers.[11] In view of these promising results, all of the phosphorothioates described here might well show significant activity and enhanced resistance to hydrolysis in a wide range of bacterial pathways that use c-di-GMP for signaling, with some diastereomers likely more effective than others. Because such phosphorothioates are attractive candidates, synthetic methods for making them are needed, and an understanding of their behavior in solution is essential.

RESULTS

Synthesis

The syntheses of all diastereomers of the mono-, di-, and trithiophosphate analogs of c-di-GMP, **5–7**, were carried out as shown in Scheme 1. This approach is based on our earlier synthesis of unmodified c-di-GMP.[8,9] The first step is coupling of the standard commercially available guanosine phosphoramidite, **1**, with the guanosine H-phosphonate monoester, **2a**, or the H-thiophosphonate monoester, **2b**. After coupling, the new phosphite triester is selectively oxidized using *tert*-butyl hydroperoxide, or sulfurized using elemental sulfur, in either case without affecting the H-phosphonate or H-thiophosphonate monoester. Detritylation is carried out using sodium bisulfate adsorbed to silica gel.[12] Approximately equal amounts of the diastereomers of **3b** or **3c** are produced by the sulfurization. The linear dimers **3a–c** are then ready for cyclization by treatment with pivaloyl chloride or diphenylchlorophosphate. Oxidation using iodine and water or sulfurization using elemental sulfur gives the cyclic derivatives **4a–e**. Sulfurization of the H-phosphonate diester produced by cyclization gives only the [R_P] diastereomer, as had been shown by Battistini for c-di-CMP.[13] Purification of the linear and cyclic dimers **3a–c** and **4a–e** was carried out on silica gel, normally without attempting to separate the diastereomers at this stage. The polar groups present, along with the mixtures of diastereomers, hampered the silica purification and lowered the yields. Deprotection of **4a–e** was carried out by treatment with methylamine in H_2O to remove the isobutyryl and cyanoethyl protecting groups, followed by desilylation using triethylamine trihydrogen fluoride. Purification of **5–7** was carried out by RP HPLC to isolate each of the diastereomers **5a**,**b**, **6a**,**b**,**c**, and **7a**,**b**. The separations were difficult, requiring repeated chromatography to get pure diastereomers, with concomitant loss of material that in some cases was significant, such that the overall yields from **2** to **5–7** did not exceed 10%.

Configuration Assignments

The only other work describing synthesis and characterization of stereochemistry of c-di-GMP monothiophosphates[10] made assignments based on a comparison of the ^{31}P NMR chemical shifts to those of the c-AMP phosphorothioates (c-AMPS), whose configuration had been established.[14] The ^{31}P NMR chemical shifts that we have found are nearly identical to the chemical shifts reported for their c-di-GMP monothiophosphates, with about a 1.5 ppm difference between the two diastereomers. In further agreement, we also found that the diastereomer with the larger ^{31}P NMR chemical shift has the shorter retention time on RP HPLC. X-ray structures of c-di-GMP[15,16] have shown the 2′-exo/3′-endo conformation typically found for RNA, and also found in cAMP.[14,17] The singlets we see in the ^{1}H NMR for the H1′ in c-di-GMP, and for all of the thioates, confirm that this is also the sugar conformation in solution.[17] The 1.5 ppm difference in ^{31}P NMR chemical shifts for the diastereomers is, however, well within the envelope of chemical shifts we have observed previously for the various complexes of c-di-GMP,[8,9] and the thioate derivatives reported here.

Further, the relationship between phosphate and nucleoside in the twelve-member ring of c-di-GMP is strikingly different from that in the six-member ring of c-AMP, as the x-ray structures demonstrate.[15,16] In cAMP the phosphate is in a rigid chair conformation directly opposite C4′,14,17 while in the larger twelve-member ring of c-di-GMP the phosphates are moved well away from C4′. Given the small chemical shift differences between the diastereomers relative to the larger chemical shift changes we have seen for different c-di-GMP complexes, and the lack of similarity of the phosphate environment between c-di-GMP and c-AMP, we chose to probe the configuration of the thiophosphate diastereomers using the now well established specificities of venom phosphodiesterase and nuclease P1.18–25 These enzymatic studies (described below) gave assignments of c-di-GMP thiophosphate configuration that are opposite to assignments based on c-AMPS.[10] We have used our enzymatic assignments for all of the compounds reported below.

The specificity of a variety of enzymes for differential cleavage of the diastereomers of linear 3′,5′-dinucleoside thiophosphates has been well known at least since Eckstein showed, by x-ray crystallography, that ribonuclease A gave exclusively the R_P diastereomer of uridine-3′-*O*-methyl ester from *endo*-uridine 2′,3′-cyclothiophosphate.[21] Our approach to the configuration assignment of the c-di-GMP monothiophosphate diastereomers was to relate their configurations to those of the corresponding linear 3′,5′-diguanosine thiophosphates, where the configuration could be established by enzymatic cleavage by venom phosphodiesterase and by nuclease P1. Venom phosphodiesterase preferentially cleaves the R_P diastereomer, while P1 preferentially cleaves the S_P diastereomer.18–25 We related results for the linear dimers to the cyclic dimers in two ways. First, as shown in Scheme 2, the linear dimers of **3b**, before detritylation, (*i*) were separated by silica chromatography. A portion of each diastereomer (***i***) was dephosphitylated[26] and deprotected to give ***ii***, which was characterized by cleavage with venom phosphodiesterase. The major portion of each separated diastereomer (***i***) was used for cyclization, followed by deprotection to give ***iii***, which was characterized by ^{31}P NMR and HPLC retention time. Thus a single linear dimer diastereomer ***i*** gave a single deprotected linear dimer ***ii*** and a single c-di-GMP monothiophosphate ***iii***. The second approach was to work back from the mixture of the diastereomers of ***iii*** (prepared without prior separation of the linear diastereomers **3b**) that were then separated by RP HPLC and characterized by ^{31}P NMR and HPLC retention time. Because nuclease P1 cleaves phosphate diesters much faster than either of the thiophosphate diastereomers, we could then use brief treatment of ***iii*** with P1 to generate the corresponding linear dimer ***iv***. As shown in Scheme 2, the linear dimers ***iv*** obtained from opening of ***iii*** have a 5′ phosphate. The presence of this phosphate should have no effect on the enzymatic cleavage of the thiophosphate. Nevertheless, we converted a portion of ***iv*** to ***ii*** by treatment of ***iv*** with bacterial alkaline phosphatase (BAP). The configuration of the linear dimers, ***ii*** and ***iv***, obtained from ***iii***, then were determined by treatment with venom phosphodiesterase as well as by treatment with nuclease P1.[27] The results of the enzymatic cleavage experiments were identical for both pathways, regardless of the source of the dimer: the c-di-GMP monothiophosphate diastereomer having the longer HPLC retention time and the smaller thiophosphate ^{31}P NMR chemical shift corresponded to the linear dimer that proved the better substrate for venom phosphodiesterase and the poorer substrate for nuclease P1, which must be the R_P diastereomer; conversely, the c-di-GMP monothiophosphate diastereomer having the shorter HPLC retention time and the larger thiophosphate ^{31}P NMR chemical shift corresponded to the linear dimer that proved the poorer substrate for venom phosphodiesterase and the better substrate for nuclease P1, which must be the S_P diastereomer. The assignments of the di- and trithioate diastereomers were then made based on their retention times and chemical shifts, as shown in Table 1, with the smaller chemical shift/longer retention time assigned the R_P configuration.

NMR Characterization

We used 1D ^{1}H and ^{31}P NMR at several temperatures to assess the polymorphism of each of the seven thioate analogs, for both the Na^{+} and K^{+} salts. We also used 2D NOESY experiments to assign the *syn* or *anti* conformation of the guanine ring relative to the ribose, based on the well-known observation that at low mixing times, *syn* arrangements give pronounced crosspeaks between the guanine H8 and the ribose H1′, while *anti* arrangements do not.[28–30] Further, we have used 2D DOSY (diffusion-ordered spectroscopy)[31–33] experiments to qualitatively evaluate relative size by means of molecular diffusion coefficients. Our previous work[9] with unmodified c-di-GMP in 0.1 M LiCl demonstrated an equilibrium among five different complexes in similar amounts (Fig 2A), four of which contain guanine quartets[34–36] (Fig 2B): a bimolecular structure, a pair of tetramolecular complexes made of two parallel guanine quartets (one all *syn* and one all *anti*), and a pair of octamolecular intercalated complexes made of four stacked quartets (one all *syn* and one all *anti*). In 0.1 M KCl, the two octamolecular complexes dominated the equilibrium. We had previously shown[8] that c-di-GMP in 0.1 M NaCl appeared to form similar complexes with stabilities somewhat like those in LiCl, but also showed signs of additional aggregation not seen with the other salts.

Partial ^{1}H NMR spectra that display the H8 region are shown in Fig 3 for both the K^{+} and Na^{+} salts of **5–7** at 30 °C. Because the H8 region is the most informative, only that section is described in this report. Spectra at lower temperatures (5 and 15 °C, not shown) display increased resonances for the less stable higher order complexes (tetra- and octamolecular) relative to the bimolecular structure, but reduced resonances for them at higher temperature (55 °C, not shown). ^{31}P NMR spectra were also acquired at multiple temperatures, shown in Fig 4 for 30 °C. Those resonances were assigned based on their temperature dependence, and relationship with the ^{1}H NMR spectra using correlations determined from our previous work with unmodified c-di-GMP.[9] Except for **6c** and **7b** (which displayed unusually poor signal to noise ratio due to extensive aggregation), the ^{31}P NMR resonances for the different forms were integrated, and the relative amounts are summarized in Table 2. 2D NOESY plots for the eight samples that display strong crosspeaks characteristic of *syn* conformations are shown in Fig. 5. The spectra for samples that did not show these characteristic *syn* crosspeaks are not shown. 2D DOSY plots for all 14 samples at 30 °C are shown in Fig. 6.

For all 14 samples at 30 °C, the H8 regions of the ^{1}H NMR spectra and the ^{31}P NMR spectra are described below, along with *syn* or *anti* determinations from the NOESY plots and, where possible, complex size based on diffusion coefficients in $m^{2}/sec \times 10^{-10}$ (D) from the DOSY plots. In our work with unmodified c-di-GMP,[9] diffusion coefficients at 30 °C for the bimolecular structure were found to be 3.3 – 3.7, those for the tetramolecular complexes were in the range of 2.0 – 2.1, and those for the octamolecular complexes were 1.8 – 1.9. (Although the mass of the octamolecular complex is twice that of the tetramolecular, its structure is more compact and therefore their diffusion coefficients are more similar than the mass difference would imply.)

Monothioates, K^{+} salts—The ^{1}H NMR spectrum of the [R_P] diastereomer **5a**, K^{+} salt (Fig 3A) displays two separate groups of octamolecular *anti* H8 resonances (D = 1.5 –1.9); two separate groups of octamolecular *syn* H8 resonances (D = 1.6 – 1.9); and no resonances with D near 3.5 for the bimolecular structure. The ^{31}P NMR spectrum (Fig 4A) displays one small resonance near −1 ppm for the phosphate of the bimolecular structure; a larger set of nearby downfield octamolecular *syn* resonances; and a larger set of nearby upfield octamolecular *anti* resonances. It has a similar pattern for the thiophosphate resonances around 55 ppm.

The ^{1}H NMR spectrum of the [S_P] diastereomer **5b**, K^{+} salt (Fig 3B) displays two separate complex groups of octamolecular *anti* H8 resonances (D = 1.5 – 1.7); one large and one small octamolecular *syn* resonance (D = 1.6 – 1.7); and a small resonance (D = 3.4) for the bimolecular

structure. The ^{31}P NMR spectrum (Fig 4B) displays one small resonance near −1 ppm for the phosphate of the bimolecular structure; a larger set of nearby downfield octamolecular *syn* resonances; and a larger set of nearby upfield octamolecular *anti* resonances. However, the pattern for the thiophosphate resonances is different, with both sets of octamolecular *syn* and *anti* resonances appearing upfield of the small resonance near 56 ppm for the bimolecular structure.

Monothioates, Na^+ salts—The ^{1}H NMR spectrum of the [R_P] diastereomer **5a**, Na^+ salt (Fig 3C) displays a group of multiple tetramolecular *anti* H8 resonances (D = 2.0 – 2.2); a group of several tetramolecular *syn* H8 resonances (D = 1.7 – 2.2); and one large broad H8 resonance for the bimolecular structure (D = 3.8). The ^{31}P NMR spectrum (Fig 4C) displays one large resonance near −1 ppm for the phosphate of the bimolecular structure; a smaller set of nearby downfield tetramolecular *syn* resonances; and a smaller set of nearby upfield tetramolecular *anti* resonances. It has a similar pattern for the thiophosphate resonances near 55 ppm.

The ^{1}H NMR spectrum of the [S_P] diastereomer **5b**, Na^+ salt (Fig 3D) displays two separate groups of tetramolecular *anti* H8 resonances (D = 2.1 – 2.4); no *syn* H8 resonances (no strong H8-H1′ NOESY crosspeaks); and two separate sharp resonances for the bimolecular structure (D = 3.7 – 3.9). The ^{31}P NMR spectrum (Fig 4D) displays one small resonance near −1 ppm for the phosphate of the bimolecular structure; and a larger set of nearby upfield tetramolecular *anti* resonances (but no downfield *syn* resonances). It has a similar pattern for the thiophosphate resonances near 56 ppm.

Summary for monothioates: Because both diastereomers of these monothioates are unsymmetrical molecules, each has two kinds of H8s, and there are different possible orientations of the monomers in any complex. This situation presumably accounts in part for the multiple H8 resonances. In spite of the resulting complexity of the spectra, several conclusions can be noted. 1) For the K^+ salts, the higher order complexes are present in much larger amounts than for the Na^+ salts (Table 2). 2) The [S_P] diastereomer in the Na^+ salt shows a larger fraction of higher order complexes than does the [R_P] diastereomer (Table 2). 3) The higher order K^+ thioates primarily have diffusion coefficients consistent with octamolecular complexes (1.5 – 1.9), while those of the Na^+ thioates primarily are consistent with tetramolecular complexes (1.8 – 2.4). 4) While both *syn* and *anti* higher order complexes are present in the K^+ thioates (with more *anti* than *syn*), in the Na^+ thioates, the [S_P] diastereomer has only *anti* complexes, while the [R_P] diastereomer has both *syn* and *anti*.

Dithioates, K^+ salts—The ^{1}H NMR spectrum of the [R_P,R_P] diastereomer **6a**, K^+ salt (Fig 3E) displays two close octamolecular *anti* H8 resonances (D = 1.8) and a third upfield octamolecular *ant*i H8 resonance (D = 1.6); two *syn* octamolecular H8 resonances (D = 1.6 – 1.7); and no resonances with D near 3.5 for the bimolecular structure. The ^{31}P NMR spectrum (Fig 4E) displays a small monothiophosphate resonance near 55 ppm for the bimolecular structure; a larger set of nearby downfield octamolecular *syn* resonances; and a larger set of nearby upfield octamolecular *anti* resonances.

The ^{1}H NMR spectrum of the [S_P,R_P] diastereomer **6b**, K^+ salt (Fig 3F) displays several broad complex octamolecular *anti* H8 resonances (D = 1.7 – 2.5); a large octamolecular *syn* H8 resonance (D = 1.7); and several small resonances for the bimolecular structure (D = 3.2 – 3.4). The ^{31}P NMR spectrum (Fig 4F) displays two small resonances for the monothiophosphates of the bimolecular structure ([R_P] near 55 ppm and [S_P] near 56 ppm); a larger set of nearby downfield octamolecular *syn* resonances; and a larger set of nearby upfield octamolecular *anti* resonances.

The ^{1}H and ^{31}P NMR spectra of the [S_P,S_P] diastereomer **6c**, K^+ salt both exhibit a poor signal to noise ratio with few resonances. This behavior is also seen (see below) for the Na^+ salt of **6c**, as well as both salt forms of **7b**, all of which have two sulfurs in the [S_p] configuration. The spectra are significantly worse at temperatures below 30°, where there are often no resonances, while heating the sample to 55° gives spectral quality comparable to the other samples at this temperature (not shown). A possible explanation is that the presence two [S_p] sulfurs promotes extensive aggregation such that only a small amount of non-aggregated material is visible at 30° C. The ^{1}H NMR spectrum (Fig 3G) displays several residual H8 resonances that are difficult to assign (D = 1.4 – 1.6); and no resonances with D near 3.5 for the bimolecular structure. Even though the NOESY was acquired at 45° C for this sample, the spectrum was not good enough to assign *syn* or *anti* conformations. The ^{31}P NMR spectrum (Fig 4G), displays a small monothiophosphate resonance near 57 ppm for the bimolecular structure; and a larger set of nearby upfield resonances (but no downfield resonances).

Dithioates, Na^+ salt—The ^{1}H NMR spectrum of the [R_P,R_P] diastereomer **6a**, Na^+ salt (Fig 3H) displays two complex groups of multiple tetramolecular *anti* H8 resonances (D = 2.0 – 2.5); two tetramolecular *syn* H8 resonances (D = 2.1 – 2.2); and two H8 resonances for the bimolecular structure (D = 3.2 – 3.3) that overlap with the upfield tetramolecular *anti* resonances but are resolved in the DOSY spectrum (Fig 6H). The ^{31}P NMR spectrum (Fig 4H) displays one large monothiophosphate resonance near 55 ppm for the bimolecular structure; a smaller set of nearby downfield tetramolecular *syn* resonances; and a smaller set of nearby upfield tetramolecular *anti* resonances.

The ^{1}H NMR spectrum of the [S_P,R_P] diastereomer **6b**, Na^+ salt (Fig 3I) displays two broad tetramolecular *anti* H8 resonances (D = 1.9 – 2.1); no *syn* H8 resonances; and two sharp H8 resonances for the bimolecular structure (D = 3.2 – 3.4). The ^{31}P NMR spectrum (Fig 4I) displays a set of two monothiophosphate resonances for the bimolecular structure ([R_P] near 55 ppm and [S_P] near 56 ppm); and one set of nearby upfield tetramolecular *anti* resonances (but no downfield *syn* resonances).

The ^{1}H NMR spectrum of the [S_P,S_P] diastereomer **6c**, Na^+ salt (Fig 3J) displays primarily one residual H8 resonance that is consistent with the bimolecular structure (D = 3.5). The ^{31}P NMR spectrum (Fig 4J) displays one monothiophosphate resonance near 57 ppm for the bimolecular structure; and a set of broad nearby upfield resonances that are difficult to assign.

Summary for dithioates: The [R_P,R_P] and [S_P,S_P] dithioates (**6a** and **6c**) are symmetrical molecules, while the [S_P,R_P] dithioate is not. The presence of multiple H8 resonances for **6a** and **6c** therefore indicates additional complexity that we are unable to define at this time. None-the-less, all four conclusions noted above for the monothioates hold true for these dithioates as well. In particular, diastereomers with one or two sulfurs in the [S_P] configuration (**5b**, **6b**, and **6c**) tend not to form *syn* complexes for the Na^+ salts, but do for the K^+ salts; and Na^+ thioates form primarily tetramolecular complexes while K^+ thioates form primarily octamolecular complexes. In addition, the presence of two sulfurs in the [S_P] configuration (**6c**) results in spectra with a poor signal to noise ratio that may be the result of extensive aggregation.

Trithioates, K^+ salt—The ^{1}H NMR spectrum of the [R_P] diastereomer **7a**, K^+ salt (Fig 3K) displays two complex groups of octamolecular *anti* H8 resonances (D = 1.6 –1.9); a large and a small octamolecular *syn* H8 resonance (D = 1.6 – 1.9); and two H8 resonances for the bimolecular structure (D = 3.1 – 3.2). The ^{31}P NMR spectrum (Fig 4K) displays one small monothiophosphate resonance near 56 ppm for the bimolecular structure; a set of larger nearby downfield octamolecular *syn* resonances; and a set of larger nearby upfield octamolecular *anti* resonances. It also has one small dithiophosphate resonance near 114 ppm for the

bimolecular structure; and two sets of larger nearby upfield octamolecular *syn* and *anti* resonances (but no nearby downfield resonances).

The ^{1}H NMR spectra of the [S_P] diastereomer **7b**, K^+ salt (Fig 3L) displays a group of multiple *anti* H8 resonances that reflect complexes that are at least as large as octamolecular (D = 1.1 – 1.3); one or two small *syn* H8 resonances (D = 1.6); and no resonances with D near 3.5 for the bimolecular structure. The NOESY was acquired at 45 °C because the signal to noise ratio was somewhat better than that at 30 °C. The ^{31}P NMR spectrum (Fig 4L) shows one small monothiophosphate resonance near 58 ppm for the bimolecular structure; and a set of larger nearby upfield *syn* and *anti* resonances (but no nearby downfield resonances). It also has one small dithiophosphate resonance near 116 ppm for the bimolecular structure; and a larger set of nearby upfield *syn* and *anti* resonances (but no nearby downfield resonances).

Trithioates, Na^+ salt—The ^{1}H NMR spectrum of the [R_P] diastereomer **7a**, Na^+ salt (Fig 3M) displays two small tetramolecular *anti* H8 resonances (D = 1.8 – 1.9); no *syn* H8 resonances; and two large H8 resonances for the bimolecular structure (D = 3.1 –3.2). The ^{31}P NMR spectrum (Fig 4M) displays one monothiophosphate resonance near 56 ppm for the bimolecular structure, and a set of nearby upfield tetramolecular *anti* resonances (but no nearby downfield resonances). It also has a dithiophosphate resonance near 114 ppm for the bimolecular structure, and a set of nearby upfield tetramolecular *anti* resonances (but no nearby downfield resonances).

The ^{1}H NMR spectrum of the [S_P] diastereomer **7b**, Na^+ salt (Fig 3N) displays two H8 resonances (D = 2.7 – 2.8) that appear to be *anti* (no strong NOESY crosspeaks), but their size is difficult to assess. The NOESY was acquired at 45 °C because the signal to noise ratio was somewhat better than that at 30 °C. The ^{31}P NMR spectrum (Fig 4N) shows a dithiophosphate resonance near 58 ppm for the bimolecular structure; and a set of nearby upfield *anti* resonances (but no nearby downfield resonances). It also has one dithiophosphate resonance near 116 ppm for the bimolecular structure; and a set of nearby upfield *anti* resonances (but no nearby downfield resonances).

Summary for trithioates: The trithioates are both unsymmetrical molecules, each with two kinds of H8s, and so have multiple possible orientations in any complex. The trends noted above also apply to these trithioates. Again, diastereomers with one or two sulfurs in the [S_P] configuration (**5b**, **6b**, **6c, 7a**, and **7b)** tend not to form *syn* complexes as the Na^+ salts, but do as the K^+ salts. Further, all the Na^+ thioates form primarily tetramolecular complexes while the K^+ thioates form primarily octamolecular complexes. In addition, the results for the [S_P] trithioate support the rationale that the presence of two sulfurs in the [S_P] configuration (**6c**, **7b**) results in extensive aggregation.

DISCUSSION

We have found that the K^+ salts of all seven thioates display more extensive higher order complex formation than do the Na^+ salts. None-the-less, 1D ^{31}P NMR always shows small amounts of the bimolecular structure in the K^+ salts, even when the less sensitive 2D DOSY cannot detect it. Although K^+ and Na^+ ions are both known to stabilize guanine quartets in nucleic acids, in general the larger and more easily dehydrated K^+ does so more effectively.[35,36] K^+ has frequently been found to be located between the planes of the quartets, whereas Na^+ is often within the planes. It is perhaps for this reason that K^+ can better stabilize the stacked quartet structures of c-di-GMP and its analogs, thereby promoting octamolecular complexes. Without this additional stabilization, tetramolecular complexes are dominant with Na^+.

We have also found that the presence of sulfur in the [S_P] configuration (**5b**, **6b**, **6c, 7a**, and **7b)** specifically stabilizes *anti* complexes and/or destabilizes *syn* complexes in the Na^+ salts, to the extent that no *syn* complexes are observed. However, for the K^+ salts, both *syn* and *anti* complexes are present. Examination of the x-ray structures[15,16] of the bimolecular form shows that the [S_P] sulfur is directed more toward the interior of the molecule, where the guanine rings are stacked, than is the [R_P]. The [S_P] sulfur may therefore be better positioned to create stabilizing interactions with key parts of the *anti* complexes and/or destabilizing clashes with parts of the *syn* complexes for the Na^+ salts.

In addition, we have found that for both the K^+ and Na^+ salts, the presence of two [S_P] sulfurs (**6c** and **7b**) gives poor spectra, perhaps as the result of extensive aggregation. This aggregation may take the form of end-to-end stacking of the tetra- or octamolecular complexes, forming extended guanine quartet structures similar to ones seen in other cases,[33,35,36] although other forms of aggregation cannot be excluded. Some of the residual resonances we do observe in the K^+ salts of **6c** and **7b**, which must reflect very low concentrations, given the poor signal to noise ratio, show diffusion coefficients that are unusually small (1.1 – 1.4), and may represent aggregates just small enough to be detected. We also note that our preliminary NMR used thioate samples with 0.1 M salts, just as in our original work on unmodified c-di-GMP.[9] However, the aggregation was so extensive that we switched to using just the stoichiometric amount, with no excess salt, for the work presented here.

CONCLUSION

Seven thiophosphate analogs of c-di-GMP were synthesized by new routes, and 1D ^1H and ^{31}P NMR, along with 2D NOESY and DOSY, were used to assess the impact of the thioate substitution(s) on the polymorphism of both the Na^+ and K^+ salts. The results demonstrate the dramatic effects of [S_P] thiophosphates, as well as major differences between the Na^+ and K^+ salts. We find that in all cases, the K^+ salts display more extensive higher order complex formation than the Na^+ salts, resulting primarily in octamolecular complexes for the K^+ salts, but tetramolecular complexes for the Na^+ salts. Further, the presence of just one [S_P] sulfur is sufficient to shift the population of the complexes entirely to the *anti* form, with no detectable *syn* complexes. The presence of two [S_P] sulfurs promotes extensive aggregation. Phosphorothioate derivatives of c-di-GMP are likely to prove useful for further exploration of the mechanisms of c-di-GMP function, where an understanding of the very different behavior of these diastereomers may be valuable.

EXPERIMENTAL

General methods

Pivaloyl chloride was freshly distilled before each use. The amidite coupling reactions were carried out in anhydrous acetonitrile that had been dried over 3Å molecular sieves. The starting materials for all reactions in dry pyridine were dried by concentration from pyridine three times.

Preparative silica gel chromatography was carried out on pre-packed silica gel flash columns from AnaLogix using gradients of methanol in CH_2Cl_2 containing 0.5% pyridine. Analytical reverse phase HPLC was carried out on a Waters 2960 system, with an Atlantis C18 column, 100Å, 4.6 mm × 50 mm, 3.0 μm. Gradients of acetonitrile and 0.1 M triethylammonium acetate (TEAA) buffer (pH 6.8) were used with a flow rate of 1.0 mL/min. ESI-MS was acquired using a Waters Micromass single quadropole LCZ system. Semi-preparative reverse phase HPLC purification was performed on a Waters Novapak C18 19 × 300 mm column using gradients of CH_3CN in 0.1 M TEAA (pH 6.8) or a Beckman ultrapore RPSC C3 10 × 250 mm column using gradients of CH_3CN in 0.1 M diisopropylethyl ammonium acetate (pH 6.8). Desalting of pure samples was performed on a Waters Novapak C18 19 × 300 mm column using gradients

of CH_3CN in 0.1 M ammonium bicarbonate. Sodium and potassium salts of **5**–**7** were obtained by ion exchange using 10 mL of AG 50W-X2 sulfonic acid resin, which had previously been converted to the Na^+ or K^+ forms, respectively.

NMR

The ^1H and ^{31}P NMR spectra were acquired on a Varian Inova 500 MHz spectrometer, with the latter referenced to neat phosphoric acid. The samples were 31 mM cyclic dimer in 0.30 mL H_2O containing 10% D_2O, pH 6.8 (adjusted with HCl or either KOH or NaOH, as appropriate). The thioates were quantified by OD measurement at 260 nm using ε = 26,100 OD M^{-1} cm^{-1}.[18]

The NOESY and DOSY spectra were acquired at 30 °C (unless otherwise noted) on a Varian Inova 500 MHz spectrometer. NOESY data were collected by 4096 (t2) times 512 (t1) complex data points with spectral widths of 8000 Hz in both dimensions. The mixing time for NOESY spectra was 150 ms, the number of scans per each t1 increment was 16, and the relaxation delay for each scan was 2 s. The DOSY spectra were collected over a spectral width of 8000 Hz using 16 scans for each of the 256 increments, with a relaxation delay of 2.5 sec and a diffusion delay of 0.1 sec. The gradient pulse strength was arrayed from 400 to 20,000. Both NOESY and DOSY acquisitions used 1 s ^1H presaturation during the relaxation delay to suppress water.

Syntheses of 2a and 2b

2-*N*-Isobutyryl-2′-*O*-*tert*-butyldimethylsilyl-3′-*O*-(H-phosphonate)-guanosine, sodium salt (2a)—To 2-*N*-isobutyryl-2′-*O*-*tert*-butyldimethylsilyl-5′-*O*-(4,4′-dimethoxytrityl)-guanosine[37,38] (3.85 g, 5.0 mmol) dissolved in 15 mL of dry pyridine was added diphenyl phosphite (1.9 mL, 10 mmol, 2 eq). After 15 min at room temperature the reaction mixture was poured into saturated $NaHCO_3$ and extracted with CH_2Cl_2 (3 × 50 mL). The organic layers were concentrated, and the residue was purified by silica gel chromatography. Product fractions were combined, concentrated to dryness, and the residue detritylated by shaking a CH_2Cl_2 solution with $NaHSO_4/SiO_2$ (1.36 g, 3.0 mmol) for 30 min. After filtration, the filtrate was evaporated with frequent addition of toluene (50 mL × 3), the last time with about 100 mL remaining. The bulk of the product was deposited on the wall of the flask, leaving the 4,4′-dimethoxytritanol in solution. Hexane (15 mL) was added to the solution, which was allowed to stand for 30 min. The liquid was decanted and the residue washed with 20 mL 15% hexane in toluene. The residue was then dissolved in CH_2Cl_2, made into a foam, and dried in a desiccator over P_2O_5 to give **2a** (2.25 g, 3.7 mmol, 74%). The product was confirmed by LC-MS in negative mode, with *m/z* (M-1) 530.4 (calcd for $C_{20}H_{33}N_5O_8PSi^-$: 530.2).

2-*N*-Isobutyryl-2′-*O*-*tert*-butyldimethylsilyl-3′-*O*-(H-thiophosphonate)-guanosine, sodium salt (2b)—To 2-*N*-isobutyryl-2′-*O*-*tert*-butyldimethylsilyl-5′-*O*-(4,4′-dimethoxytrityl)-guanosine[37,38] (3.21 g, 4.1 mmol) dissolved in 15 mL of dry pyridine was added diphenylphosphite (1.6 mL, 8.2 mmol, 2 eq). After 15 min lithium sulfide (Li_2S, 0.94 g, 20.5 mmol, 5 eq) was added. After 40 min, the mixture was poured into saturated $NaHCO_3$ and extracted with CH_2Cl_2 (3 × 50 mL). The organic layers were concentrated and the residue was purified by silica gel chromatography. Product fractions were combined, concentrated to dryness and the residue dissolved in CH_2Cl_2. Detritylation occurred on standing overnight and the product was separated from 4,4′-dimethoxytritanol as described for **2a** to give the H-thiophosphonate **2b** (1.81 g, 2.9 mmol, 71%). The product was confirmed by LC-MS in negative mode, with *m/z* (M-1) 546.4 (calcd for $C_{20}H_{33}N_5O_7PSSi^-$: 546.2).

Synthesis of the [R_P] monothiophosphate (c-GpGps) (5a)

2-*N*-Isobutyryl-2′-*O*-*tert*-butyldimethylsilyl-guanosinylyl (3′→5′)-2-*N*-isobutyryl-2′-*O*-*tert*-butyldimethylsilyl-3′-*O*-(H-phosphonate)-guanosine, sodium salt (3a)—To a mixture of phosphoramidite **1** (1.45 g, 1.5 mmol, 1.5 eq) and H-phosphonate **2a** (0.61g, 1.0 mmol) dissolved in 20 mL CH_3CN at room temperature was added pyridinium trifluroacetate (0.58 g, 3 mmol, 2 eq to **1**). The mixture was stirred for 30 min, followed by addition of anhydrous *tert*-butylhydroperoxide (0.87 mL, 6.25 mmol) in decane. After 30 min, the mixture was poured into aqueous $NaHCO_3$ and extracted with ethyl acetate. The organic layers were then concentrated and purified to >80% purity by silica gel chromatography. The product fractions were concentrated to dryness, the residue dissolved in CH_2Cl_2 and treated with $NaHSO_4/SiO_2$ (0.91 g), and the product isolated as described above for **2a** to give 0.64 g crude **3a** as a mixture of two unresolved diastereomers. The **3a** mixture was confirmed by LC-MS in negative mode, with *m/z* (M−1) 1113.0 (calcd for $C_{43}H_{68}N_{11}O_{16}P_2Si_2^-$: 1112.4).

Cyclo-2-*N*-isobutyryl-2′-*O*-*tert*-butyldimethylsilyl-P-guanosinylyl-(3′→5′)-2-*N*-isobutyryl-2′-*O*-*tert*-butyldimethylsilyl-[R_P]-P-thioguanosinylyl-(3′→5′), sodium salt (4a)—To a solution of a portion of crude **3a** from above (0.28 g) in 15 mL dry pyridine was added pivaloyl chloride (Pv-Cl, 0.12 mL, 1.0 mmol). After 3 min, elemental sulfur (40 mg, 1.25 mmol) was added, and the reaction was stirred for 40 min. The mixture was then concentrated, evaporated with toluene three times and CH_3CN three times, filtered to remove excess sulfur, and concentrated to dryness to give crude **4a** (0.25 g). The residue was not further purified before deprotection, which is described below. **4a** in the residue was confirmed by LC-MS in negative mode, with *m/z* (M-1) 1127.1 (calcd for $C_{43}H_{66}N_{11}O_{15}P_2SSi_2^-$: 1126.4).

Cyclo-P-guanosinylyl (3′→5′)-[R_P]-P-thioguanosinylyl-(3′→5′), ammonium salt (c-GpGps [R_P], 5a)—To the crude **4a** from above (0.25 g) was added 4 mL of methylamine in water (40%). After 40 min the mixture was concentrated and evaporated with pyridine three times to remove water. To the residue was added TEA•3HF (2.2 mL, 13.3 mmol) and an additional 1.5 mL TEA. After being heated at 50 °C for 4 hrs, the reaction was quenched with 7 mL isopropyl trimethylsilyl ether.[39] Ethyl ether (10 mL) was added to complete precipitation of **5a**. The mixture was allowed to stand overnight, the supernatant was decanted, and the product purified by semi-preparative RP HPLC on a Waters Novapak C18 column using a gradient of 2–20% CH_3CN in 0.1 M TEAA over 90 min. The pure fractions were pooled, lyophilized, and desalted by C18 RP-HPLC using a gradient of CH_3CN in 0.1 M ammonium bicarbonate to give pure **5a** (12 μmol, 3% from **2a**). **5a** was confirmed by LC-MS in negative mode, with *m/z* (M-1) 705.3 (calcd for $C_{20}H_{23}N_{10}O_{13}P_2S^-$: 705.1).

Synthesis of the [R_P] (5a) and [S_P] (5b) monothiophosphates (c-GpsGp)

2-*N*-Isobutyryl-2′-*O*-*tert*-butyldimethylsilyl-P-thioguanosinylyl (3′→5′)-2-*N*-isobutyryl-2′-*O*-*tert*-butyldimethylsilyl-3′-*O*-(H-phosphonate)-guanosine, sodium salt (3b)—To a mixture of phosphoramidite **1** (1.45 g, 1.5 mmol, 1.7 eq) and H-phosphonate **2a** (0.54 g, 0.90 mmol) dissolved in 20 mL CH_3CN at room temperature was added pyridinium trifluroacetate (0.58 g, 3.0 mmol, 2 eq to **1**). After 30 min, elemental sulfur (0.16 g, 5.0 mmol) dissolved in 30 mL 1:1 pyridine:CH_2Cl_2 was added, and the mixture was stirred for 40 min. The mixture was then concentrated, evaporated with toluene three times and CH_3CN three times, filtered to remove excess solid sulfur, and concentrated to dryness. The residue was purified to >80% purity by silica gel chromatography. The product fractions were concentrated to dryness, the residue dissolved in CH_2Cl_2 and treated with $NaHSO_4/SiO_2$ (0.91 g) as described above for **2a** to give 0.72 g of crude **3b** as a mixture of two partially resolved diastereomers. The **3b** mixture was confirmed by LC-MS in negative mode, with *m/z* (M−1) 1128.9 (calcd for $C_{43}H_{68}N_{11}O_{15}P_2SSi_2^-$:1128.4).

Cyclo-2-*N*-isobutyryl-2′-*O*-*tert*-butyldimethylsilyl-P-thioguanosinylyl (3′→5′)-2-*N*-isobutyryl-2′-*O*-*tert*-butyldimethylsilyl-P-guanosinylyl-(3′→5′), sodium salt (4b)—To a solution of a portion of crude **3b** from above (0.41 g) in 15 mL dry pyridine was added Pv-Cl (0.17 mL, 1.4 mmol). After 3 min, water (0.10 mL, 5.6 mmol, 4 eq to Pv-Cl) was added, followed by iodine (0.432 g, 1.7 mmol). After 5 min the mixture was poured into aqueous $NaHCO_3$ containing Na_2SO_3 (0.34 g) and extracted using CH_2Cl_2. The organic layers were concentrated with addition of toluene three times and purified to >80% purity by silica gel chromatography to give crude **4b** (0.14 g) as a mixture of two partially resolved diastereomers. The **4b** mixture was confirmed by LC-MS in negative mode, with *m/z* (M-1) 1126.7 (calcd for $C_{43}H_{66}N_{11}O_{15}P_2SSi_2^-$: 1126.4).

Cyclo-[R_P]-P-thioguanosinylyl (3′→5′)-P-guanosinylyl-(3′→5′), ammonium salt (c-GpsGp [R_P], 5a) and cyclo-[S_P]-P-thioguanosinylyl (3′→5′)-P-guanosinylyl-(3′→5′), ammonium salt (c-GpsGp [S_P], 5b)—The crude mixture of two diastereomers of **4b** from above (0.14 g) was treated in the same way as the single diastereomer **4a**. C18 RP-HPLC using 0.1 M TEAA buffer and CH_3CN gave two major fractions, each containing **5a** or **5b** as the major component. Fractions from each peak were combined, further purified by C18 RP-HPLC using a different gradient, and then desalted to give pure **5a** (18 μmol, 3% from **2a**) and **5b** (10 μmol, 2% from **2a**). **5a** had the same LC-MS profile as above, and **5b (**with a different retention time, Table 1) was confirmed by LC-MS in negative mode, with *m/z* (M-1) 705.3 (calcd for $C_{20}H_{23}N_{10}O_{13}P_2S^-$: 705.1).

Synthesis of the [R_P,R_P] (6a) and [S_P,R_P] (6b) dithiophosphates (c-GpsGps)

Cyclo-2-*N*-isobutyryl-2′-*O*-*tert*-butyldimethylsilyl-P-thioguanosinylyl (3′→5′)-2-*N*-isobutyryl-2′-*O*-*tert*-butyldimethylsilyl-P-thioguanosinylyl-(3′→5′), sodium salt (4c)—To a solution of a portion of crude **3b** from above (0.29 g) dissolved in 15 mL dry pyridine was added Pv-Cl (0.10 mL, 0.8 mmol). After 3 min, elemental sulfur (25.6 mg, 0.8 mmol) was added, and the reaction was stirred for 40 min. The mixture was then concentrated, evaporated with toluene three times and CH_3CN three times, filtered to remove excess sulfur, and concentrated to dryness to give crude **4c** (0.22 g) as a mixture of two partially resolved diastereomers. The residue was not further purified before deprotection, which is described below. The **4c** mixture was confirmed by LC-MS in negative mode, with *m/z* (M-1) 1142.9 (calcd for $C_{43}H_{66}N_{11}O_{14}P_2S_2Si_2^-$: 1142.3).

Cyclo-[R_P]-P-thioguanosinylyl (3′→5′)-[R_P]-P-thioguanosinylyl-(3′→5′), ammonium salt (c-GpsGps [R_P,R_P], 6a) and cyclo-[S_P]-P-thioguanosinylyl (3′→5′)-[S_P]-P-thioguanosinylyl-(3′→5′), ammonium salt (c GpsGps [S_P,R_P], 6b)—The crude mixture of two diastereomers of **4c** from above (0.22 g) was deprotected as described for **4a**. C18 RP-HPLC using 0.1 M TEAA buffer and CH_3CN resolved the mixture into two major fractions, each containing **6a** or **6b** as the major component. The fractions for each diastereomer were pooled, lyophilized and individually further purified by C18 RP-HPLC, and then desalted to give pure **6a** (29 μmol, 3% from **2a**) and **6b** (16 μmol, 2% from **2a**). These were characterized by LC-MS with different retention times (Table 1) and *m/z* (M-1) of 721.6 for **6a** and 721.5 for **6b** (calcd for $C_{20}H_{23}N_{10}O_{12}P_2S_2^-$: 721.0).

Synthesis of the [R_P,R_P] (6a), [S_P,R_P] (6b), and [S_P,S_P] (6c) dithiophosphates (c-GpsGps)

2-*N*-Isobutyryl-2′-*O*-*tert*-butyldimethylsilyl-P-thioguanosinylyl (3′→5′)-2-*N*-isobutyryl-2′-*O*-*tert*-butyldimethylsilyl-3′-*O*-(H-thiophosphonate)-guanosine, sodium salt 3c—To a mixture of phosphoramidite **1** (5.81 g, 6.0 mmol, 1.5 eq) and H-thiophosphonate **2b** (2.52 g, 4.0 mmol) dissolved in 40 mL CH_3CN was added pyridinium trifluroacetate (2.31 g, 12 mmol, 2 eq to **1**). The mixture was stirred for 30 min, followed by addition of elemental sulfur (0.384 g, 12 mmol) dissolved in 30 mL 1:1 pyridine:CH_2Cl_2. After

40 min, the mixture was concentrated and evaporated with toluene three times and CH_3CN three times, filtered to remove excess sulfur, and concentrated to dryness. The residue was purified to >80% purity by silica gel chromatography. The product fractions were concentrated to dryness, the residue dissolved in CH_2Cl_2 and treated with $NaHSO_4/SiO_2$ (2.73 g) as described above for **2a** to give 2.33 g of crude **3c** as a partially resolved mixture of diastereomers. The **3c** mixture was confirmed by LC-MS in negative mode, with *m/z* (M-1) of 1144.8 (calcd for $C_{43}H_{68}N_{11}O_{14}P_2S_2Si_2^-$: 1144.3).

Cyclo-2-*N*-isobutyryl-2′-*O*-*tert*-butyldimethylsilyl-P-thioguanosinylyl (3′→5′)-2-*N*-isobutyryl-2′-*O*-*tert*-butyldimethylsilyl-P-thioguanosinylyl-(3′→5′), sodium salt 4d)—To a solution of a portion of crude **3c** from above (0.41g) in 20 mL of dry pyridine was added diphenyl chlorophosphate (DPP-Cl, 0.1 mL, 0.5 mmol) dissolved in 3 mL pyridine. After 20 min, H_2O (12 μL, 0.67 mmol) was added, followed by I_2 (0.42 g, 1.65 mmol). After 5 min the mixture was poured into aqueous $NaHCO_3$ containing Na_2SO_3 (0.34 g) and extracted with CH_2Cl_2. The organic layers were concentrated with addition of toluene three times and then purified to >80% purity by silica gel chromatography to give crude **4d** (0.21 g) as a partially resolved mixture of three diastereomers. The **4d** mixture was confirmed by LC-MS in negative mode, with *m/z* (M-1) of 1142.3 (calcd for $C_{43}H_{66}N_{11}O_{14}P_2S_2Si_2^-$: 1142.3).

Cyclo-[R_P]-P-thioguanosinylyl (3′→5′)-[R_P]-P-thioguanosinylyl-(3′→5′), ammonium salt (c-GpsGps [R_P,R_P], 6a), cyclo-[S_P]-P-thioguanosinylyl (3′→5′)-[R_P]-P-thioguanosinylyl-(3′→5′), ammonium salt (c GpsGps [S_P,R_P], 6b), and cyclo-[S_P]-P-thioguanosinylyl (3′→5′)-[S_P]-P-thioguanosinylyl-(3′→5′), ammonium salt (c-GpsGps [S_P,S_P], 6c)—The crude mixture of three diastereomers of **4d** from above (0.21 g) was deprotected as described for **4a**. C18 RP-HPLC using 0.1 M TEAA buffer and CH_3CN gave three major fractions, each containing **6a**, **6b**, or **6c** as the major component. The fractions containing **6a** and **6b** were further purified by C18 RP-HPLC, and the fractions containing **6c** were further purified on a Beckman C3 column. Desalting gave pure **6a** (25μmol, 4% from **2b**), **6b** (12 μmol, 2% from **2b**), and **6c** (4μmol, 1% from **2b**). **6a** and **6b** had the same LC-MS profiles as above, and **6c** (with a different retention time, Table 1) was confirmed by LC-MS in negative mode, with *m/z* (M-1) 721.4 (calcd for $C_{20}H_{23}N_{10}O_{12}P_2S_2^-$: 721.0).

Synthesis of the [R_P] (7a) and [S_P] (7b) trithiophosphates (c-GpsGpss)

Cyclo-2-*N*-isobutyryl-2′-*O*-*tert*-butyldimethylsilyl-P-thioguanosinylyl (3′→5′)-2-*N*-isobutyryl-2′-*O*-*tert*-butyldimethylsilyl-P-dithioguanosinylyl-(3′→5′), sodium salt (4e)—To a solution of a portion of crude **3c** from above (0.85 g) dissolved in 20 mL dry pyridine was added DPP-Cl (0.22 mL, 1.05 mmol) dissolved in 3 mL pyridine. After 20 min, elemental sulfur (0.068 g, 2.1 mmol) was added, and the mixture was stirred for 40 min. The mixture was concentrated, evaporated with toluene three times and CH_3CN three times, filtered to remove excess sulfur, and concentrated to dryness. The residue was purified to >80% purity by silica gel chromatography to give crude **4e** (0.85 g) as a mixture of two partially resolved diastereomers. The **4e** mixture was confirmed by LC-MS in negative mode, with *m/z* (M-1) 1158.7 (calcd for $C_{43}H_{66}N_{11}O_{13}P_2S_3Si_2^-$: 1158.3).

Cyclo-[R_P-P-thioguanosinylyl (3′→5′)-P-dithioguanosinylyl-(3′→5′), ammonium salt (c-GpsGpss [R_P], 7a) and cyclo-[S_P]-P-thioguanosinylyl (3′→5′)-P-dithioguanosinylyl-(3′→5′), ammonium salt (c-GpsGpss [S_P], 7b)—A portion of the crude mixture of two diastereomers of **4e** from above (0.52 g) was deprotected as described for **4a**. C18 RP-HPLC using 0.1 M TEAA buffer and CH_3CN gave two major fractions, each containing **7a** or **7b** as the major component. The fractions containing **7a** were further purified by C18 RP-HPLC, and the fractions containing **7b** were further purified on a Beckman C3

column. Desalting gave pure **7a** (32μmol, 4% from **2b**) and **7b** (6 μmol, 1% from **2b**). The products had different retention times (Table 1) and were confirmed by LC-MS in negative mode, with *m/z* (M-1) 737.4 for **7a** and 737.1 for **7b** (calcd for $C_{20}H_{23}N_{10}O_{11}P_2S_3^-$: 737.0).

Enzymatic Cleavage Experiments

Preparation of *ii*—To ***i*** (0.2 g, 0.13 mmol) dissolved in 9 mL of dry pyridine and ethylene glycol (0.08 g, 1.3 mmol, 10 eq) was added adamantoyl chloride (0.13 g, 0.65 mmol, 5 eq). After 3 hrs, the reaction was quenched with saturated $NaHCO_3$ and extracted three times with CH_2Cl_2. The organic layers were combined and concentrated. To the residual oil was added 5 mL of aq 40 % methylamine. After 1 hr the mixture was dried by concentration from pyridine three times. To the residue was added TEA·3HF (1.8 mL, 11 mmol, 125 eq to TBS) and 1.4 mL TEA. After 4 hrs at 50 °C, the reaction was quenched with 5.4 mL isopropyl trimethylsilyl ether and the product collected by centrifugation. To the residue was added 7 mL of 0.5 M acetic acid. After 18 h the mixture was concentrated, the residue dissolved in H_2O, and the solution washed with ethyl ether three times. The aqueous layers were concentrated, and the residue was purified by semi-preparative RP HPLC.

SVPD cleavage of *ii*—To 5 OD (0.20 μmol) of ***ii*** dissolved in 250 μL buffer (pH 7.0) containing 100 mM Tris-Cl and 2 mM $MgCl_2$ was added 0.003 units of SVPDE. The solution was maintained at 37° C, with 10 μL aliquots analyzed by RP-HPLC over 80 h. The percentage of remaining linear dimer was determined by integration of the corresponding peak in the chromatograms.

P1, BAP, and SVPD cleavage of *iii*—To 6 OD (0.23 μmol) of ***iii*** dissolved in 600 uL TEAA buffer (pH 7.0) was added 0.30 units of nuclease P1. The solution was maintained at 37° C with 15 μL aliquots analyzed by RP-HPLC to monitor the disapperance of cyclic dimer. After the completion of ring-opening, the solution was heated at 95° C for 30 min. After cooling to room temperature, 2.0 units of BAP were added, and the removal of 5′-phosphate was monitored by HPLC by injection of 15 μL aliquots. After completion of dephosphorylation, the mixture was heated at 95° C for 30 min. After cooling to room temperature, 0.004 units of SVPDE were added. The mixture was maintained at 37° C with 15 μL aliquots analyzed by HPLC over 40 h.

P1 and SVPD cleavage of *iii*—To 6 OD (0.23 μmol) of ***iii*** dissolved in 600 uL TEAA buffer (pH 7.0) was added 0.30 units of nuclease P1. The solution was maintained at 37° C with 15 μL aliquots analyzed by RP-HPLC to monitor the disapperance of cyclic dimer. After the completion of ring-opening, the solution was heated at 95° C for 30 min. After cooling to room temperature, the solution was divided into two equal parts. To one was added 0.001 units of SVPDE. The mixture was maintained at 37° C with 15 μL aliquots analyzed by HPLC over 47 h.

P1 cleavage of *iii*—The pH of the second part above was adjusted to between 5 and 6 using acetic acid and 0.25 units of nuclease P1 was added. The solution was maintained at 37° C with 15 μL aliquots analyzed by HPLC over 50 h.

Acknowledgments

This work was supported by NIH grant GM079760.

References

1. Romling U, Amikam D. Cyclic di-GMP as a second messenger. Current Opinion in Microbiology 2006;9:218–228. [PubMed: 16530465]

2. Jenal U, Malone J. Mechanisms of cyclic-di-GMP signaling in bacteria. Annual Review of Genetics 2006;40:385–407.
3. Cotter PA, Stibitz S. c-di-GMP-mediated regulation of virulence and biofilm formation. Current Opinion in Microbiology 2007;10:17–23. [PubMed: 17208514]
4. Tamayo R, Pratt JT, Camilli A. Roles of cyclic diguanylate in the regulation of bacterial pathogenesis. Annual Review of Microbiology 2007;61:131–148.
5. Karaolis DKR, Means TK, Yang D, Takahashi M, Yoshimura T, Muraille E, Philpott D, Schroeder JT, Hyodo M, Hayakawa Y, Talbot BG, Brouillette E, Malouin F. Bacterial c-di-GMP is an immunostimulatory molecule. Journal of Immunology 2007;178:2171–2181.
6. Karaolis DKR, Newstead MW, Zeng X, Hyodo M, Hayakawa Y, Bhan U, Liang H, Standiford TJ. Cyclic di-GMP stimulates protective innate immunity in bacterial pneumonia. Infection and Immunity 2007;75:4942–4950. [PubMed: 17646358]
7. Kline T, Jackson SR, Deng W, Verlinde CLMJ, Miller SI. Design and synthesis of bis-carbamate analogs of cyclic bis-(3′-5′)-diguanylic acid (c-di-GMP) and the acyclic dimer PGPG. Nucleosides, Nucleotides & Nucleic Acids 2008;27:1282–1300.
8. Zhang Z, Gaffney BL, Jones RA. c-di-GMP displays a monovalent metal ion-dependent polymorphism. Journal of the American Chemical Society 2004;126:16700–16701. [PubMed: 15612689]
9. Zhang Z, Kim S, Gaffney BL, Jones RA. Polymorphism of the signaling molecule c-di-GMP. Journal of the American Chemical Society 2006;128:7015–7024. [PubMed: 16719482]
10. Ross P, Mayer R, Weinhouse H, Amikam D, Huggirat Y, Benziman M, Vroom Ed, Fidder A, Paus Pd, Sliedregt LAJM, Marel GAvd, Boom JHv. The cyclic diguanylic acid regulatory system of cellulose synthesis in *Acetobacter xylinum*. Journal of Biological Chemistry 1990;265:18933–18943. [PubMed: 2172238]
11. Hyodo M, Sato Y, Hayakawa Y. Synthesis of cyclic bis(3′-5′)diguanylic acid (c-di-GMP) analogs. Tetrahedron 2006;62:3089–3094.
12. Das B, Mahender G, Kumar VS, Chowdhury N. Chemoselective deprotection of trityl ethers using silica-supported sodium hyudrogen sulfate. Tetrahedron Letters 2004;45:6709–6711.
13. Battistini C, Fustinoni S, Brasca MG, Borghi D. Stereoselective synthesis of cyclic dinucleotide phosphorothioates. Tetrahedron 1993;49:1115–1132.
14. Baraniak J, Kinas RW, Lesiak K, Stec W. Stereospecific synthesis of adenosine 3′,5′-(Sp)- and -(Rp)-cyclic phosphorothioates (cAMPs). Chemical Communications 1979:940–941.
15. Egli M, Gessner RV, Williams LD, Quigley GJ, van der Marel GA, van Boom JA, Rich A, Frederick CA. Atomic-resolution strucure of the cellulose synthase regulator cyclic diguanylic acid. Proceedings of the National Academy of Sciences U S A 1990;87:3235–3239.
16. Guan Y, Gao YG, Liaw YC, Robinson H, Wang AHJ. Molecular structure of cyclic diguanylic acid at 1A resoltuion of two crystal forms: self-association, interactions with metal ion/planar dyes and modeling studies. Journal of Biomolecular Structure & Dynamics 1993;11:253–276. [PubMed: 8286055]
17. Robins MJ, MacCoss M. Nucleic acid related compounds. 26. A “Geometry-only” method for determining the anomeric configuration of nucleosides based on the H-1′ NMR signal of cyclic α and β 3′,5′-mononucleotides. Journal of the American Chemical Society 1977;99:4654–4660. [PubMed: 874228]
18. Burgers PMJ, Eckstein F. Absolute configuration of the diastereomers of adenosine 5′-O-(1-thiotriphosphate): consequences for the stereochemistry of polymereization by DNA-dependent RNA polymerase from *Escherichia coli*. Proceedings of the National Academy of Sciences, USA 1978;75:4798–4800.
19. Bryant FR, Benkovic SJ. Stereochemical course of the reaction catalyzed by 5′-nucleotide phosphodiesterase from snake venom. Biochemistry 1979;18:2825–2828. [PubMed: 224905]
20. Eckstein F. Phosphorothioate analogues of nucleotides. Accounts of Chemical Research 1979;12:204–210.
21. Saenger W, Suck D, Eckstein F. On the mechanism of ribonuclease A. European Journal of Biochemistry 1974;46:559–567. [PubMed: 4853455]

22. Griffiths AD, Potter BVL, Eperon IC. Stereospecificity of nucleases towards phosphorothioate-substituted RNA: stereochemistry of transcription by T7 RNA polymerase. Nucleic Acids Research 1987;15:4145–4162. [PubMed: 2438652]
23. Potter BVL, Connolly BA, Eckstein F. Synthesis and configurational analysis of a dinucleoside phosphate isotopically chiral at phosphorus. Stereochemical course of *Penicillium citrum* nclease P1 reaction. Biochemistry 1983;22:1369–1377. [PubMed: 6301546]
24. Usher DA, Erenrich ES, Eckstein F. Geometry of the first step in the action of ribonuclease-A. Proceedings of the National Academy of Sciences, USA 1972;69:115–118.
25. Slim G, Gait MJ. Configurationally defined phosphorothioate-containing oligoribonucleotides in the study of the mechanism of cleavage of hammerhead ribozymes. Nucleic Acids Research 1991;19:1183–1188. [PubMed: 1709484]
26. Wang W, Song Q, Jones RA. Nucleoside recovery in DNA and RNA synthesis. Tetrahedron Letters 1999;40:8971–8974.
27. Zhao, J. PhD thesis. Rutgers University; 2009. Synthesis and characterization of seven thiophosphate analogs of cyclic diguanosine monophosphate.
28. Smith FW, Feigon J. Quadruplex structure of *Oxytricha* telomeric DNA oligonucleotides. Nature (London) 1992;356:164–1168. [PubMed: 1545871]
29. Wang KY, McCurdy S, Shea RG, Swaminathan S, Bolton PH. A DNA aptamer which binds to and inhibits thrombin exhibits a new structural motif for DNA. Biochemistry 1993;32:1899–1904. [PubMed: 8448147]
30. Wang Y, de los Santos C, Gao X, Greene K, Live D, Patel DJ. Multinuclear nuclear magnetic resonance studies of Na cation-stabilized complex formed by d(GGTTTTCGG) in solution. Journal of Molecular Biology 1991;222:819–832. [PubMed: 1660934]
31. Asadi A, Patrick BO, Perrin DM. G^C quartet - a DNA-inspired Janus-GC heterocycle: synthesis, structural analysis, and self-organization. Journal of the American Chemical Society 2008;130:12860–12861. [PubMed: 18767852]
32. Wong A, Ida R, Spindler L, Wu G. Disodium guanosine 5′-monophosphate self-associates into nanoscale cylinders at pH 8: a combined diffusion NMR spectroscopy and dynamic light scattering study. Journal of the American Chemical Society 2005;127:6990–6998. [PubMed: 15884942]
33. Wu G, Kwan ICM. Helical structure of disodium 5′-guanosine monophosphate self-assembly in neutral solution. Journal of the American Chemical Society 2009;131:3180–3182.
34. Davis JT. G-quartets 40 years later: from 5′GMP to molecuclar biology and supramolecular chemistry. Angewandte Chemie, International Edition in English 2004;43:668–698.
35. Hardin CC, Perry AG, White K. Thermodynamic and kinetic characterization of the dissociation and assembly of quadruplex nucleic acids. Biopolymers (Nucleic Acid Sciences) 2001;56:147–194. [PubMed: 11745110]
36. Keniry MA. Quadruplex structures in nucleic acids. Biopolymers (Nucleic Acid Sciences) 2001;56:123–146. [PubMed: 11745109]
37. Serebryany V, Beigelman L. An efficient preparation of protected ribonucleosides for phosphoramidite RNA synthesis. Tetrahedron Letters 2002;43:1983–1985.
38. Furusawa K, Ueno K, Katsura T. Synthesis and restricted conformation of 3′,5′-O-(di-t-butylsilanediyl)ribonucleosides. Chemistry Letters 1990:97–100.
39. Song Q, Jones RA. Use of silyl ethers as fluoride scavengers in RNA synthesis. Tetrahedron Letters 1999;40:4653–4654.

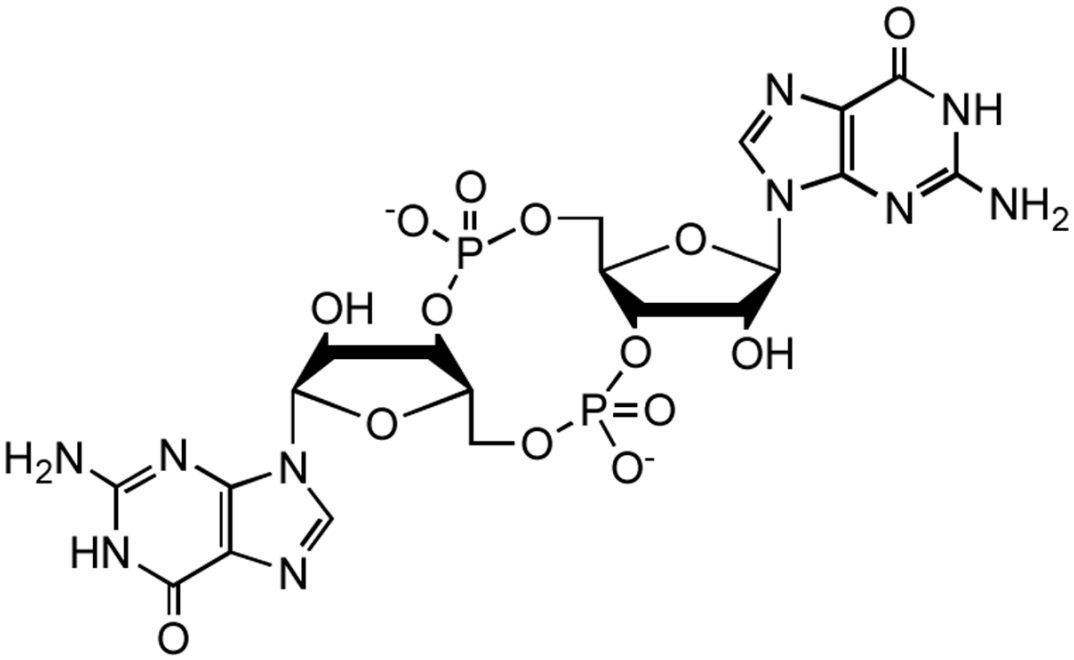

Figure 1.

Fig 2A

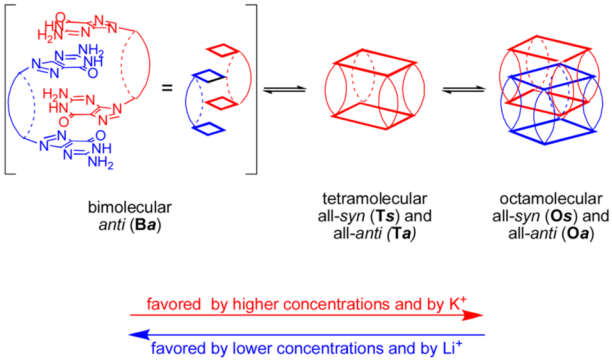

Fig 2B

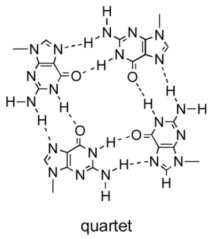

Figure 2.

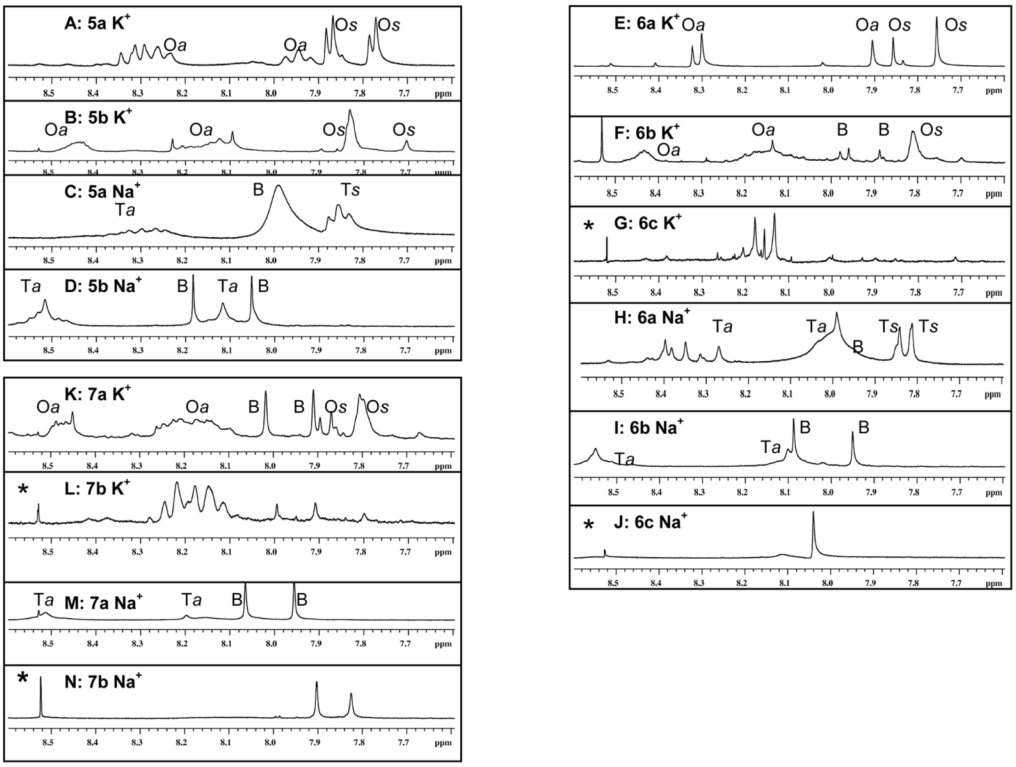

Fig 3.

^{1}H NMR spectra (H8 region) for **5**, **6**, and **7** at 30 °C (*a* = *anti*, *s* = *syn*, B = bimolecular, T = tetramolecular, O = octamolecular, * = residual resonances associated with extreme aggregation)

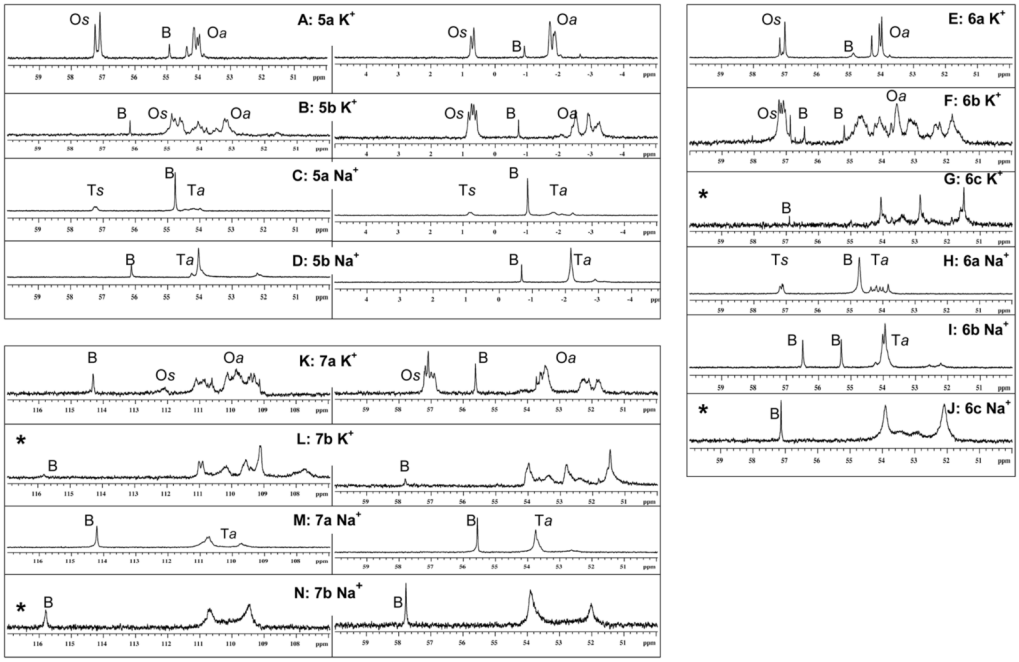

Fig 4.

^{31}P NMR spectra for **5**, **6**, and **7** at 30 °C (*a* = *anti*, *s* = *syn*, B = bimolecular, T = tetramolecular, O = octamolecular, *= residual resonances associated with extreme aggregation)

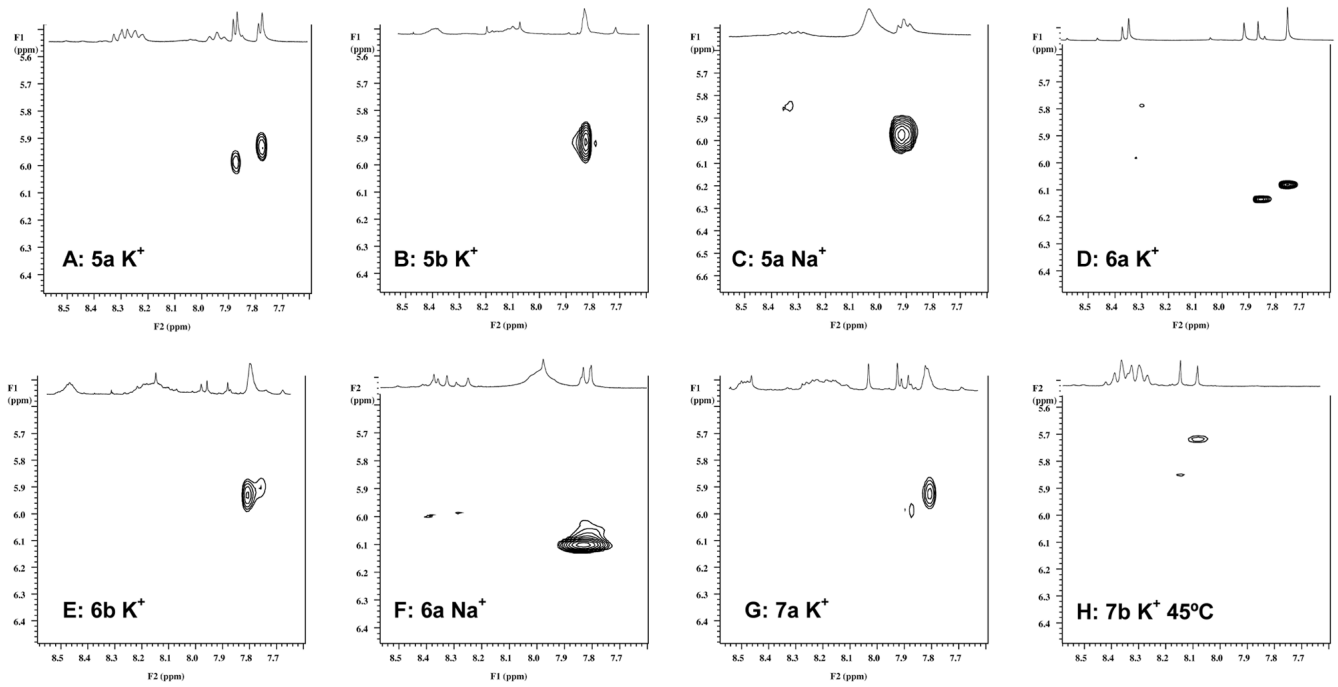

Fig 5.

2D NOESY plots for the H8/H1′ region for **5a** K^+, **5b** K^+, **5a** Na^+, **6a** K^+, **6b** K^+, **6a** Na^+ and **7a** K^+, all at 30 °C, and **7b** K^+ at 45 °C, all showing the H8/H1′ crosspeaks of *syn* conformations. Not shown: plots for **5b** Na^+, **6b** Na^+, and **7a** Na^+ which displayed good signal/noise ratio at 30 °C, but no H8/H1′ crosspeaks, or plots of **6c** Na^+ and **7b** Na^+ which only displayed good signal/noise ratio at 45 °C because of extensive aggregation, but no H8/H1′ crosspeaks. A plot for **6c** K^+ did not show good signal/noise ratio even at 45 °C.

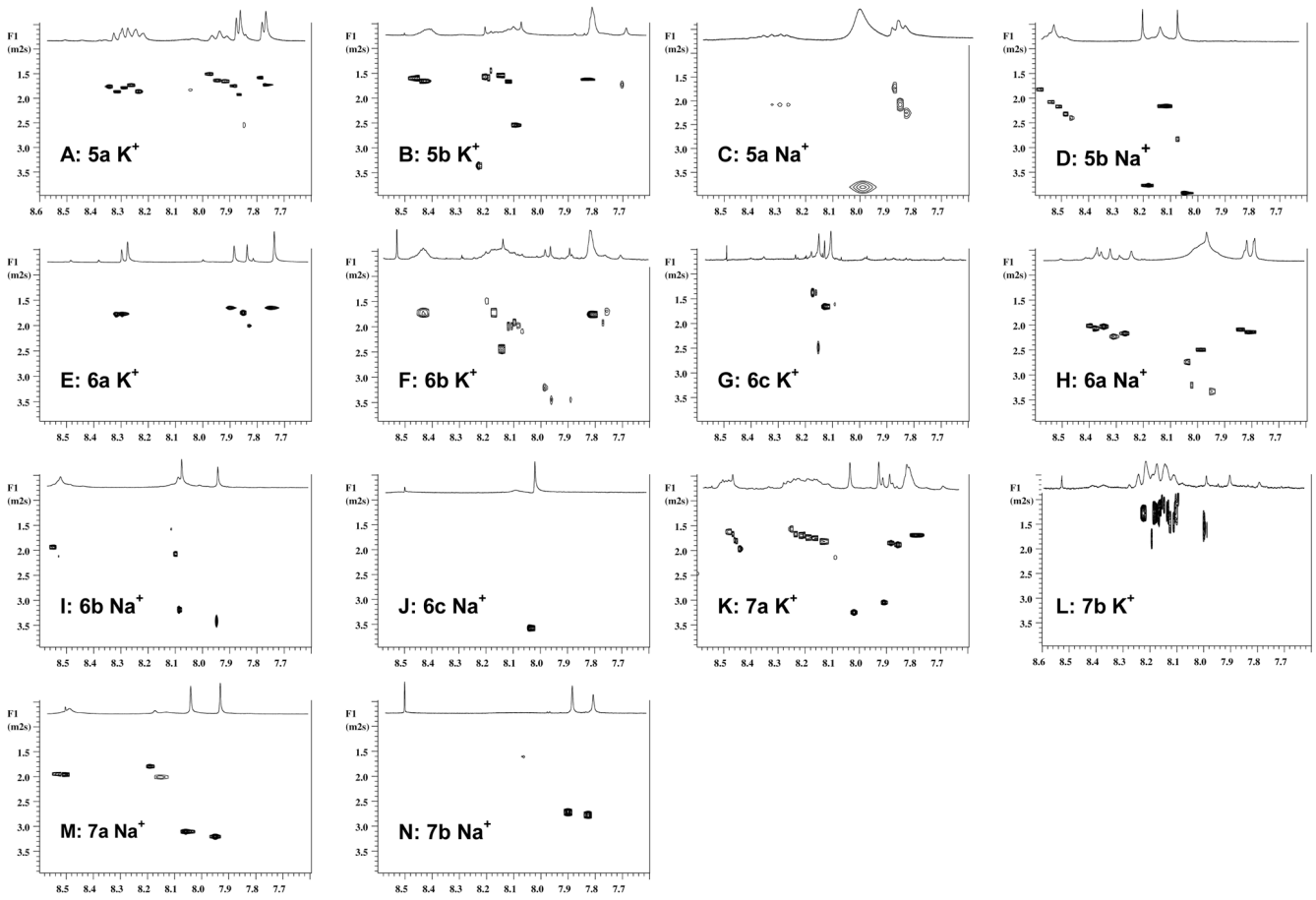

Fig 6.
2D DOSY spectra at 30 °C for all samples, with diffusion coefficients (D) displayed on the vertical axes in $m^2/sec \times 10^{-10}$

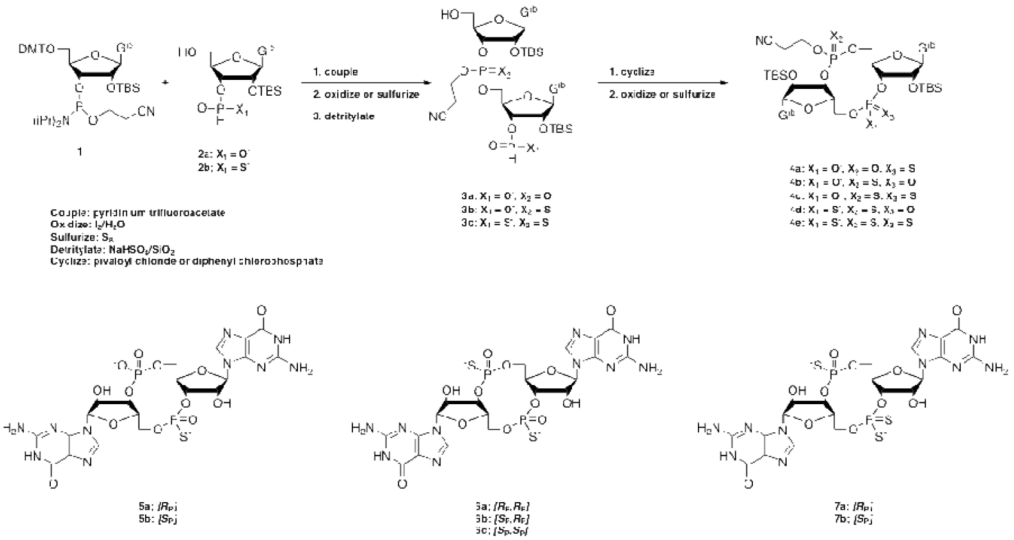

Scheme 1.

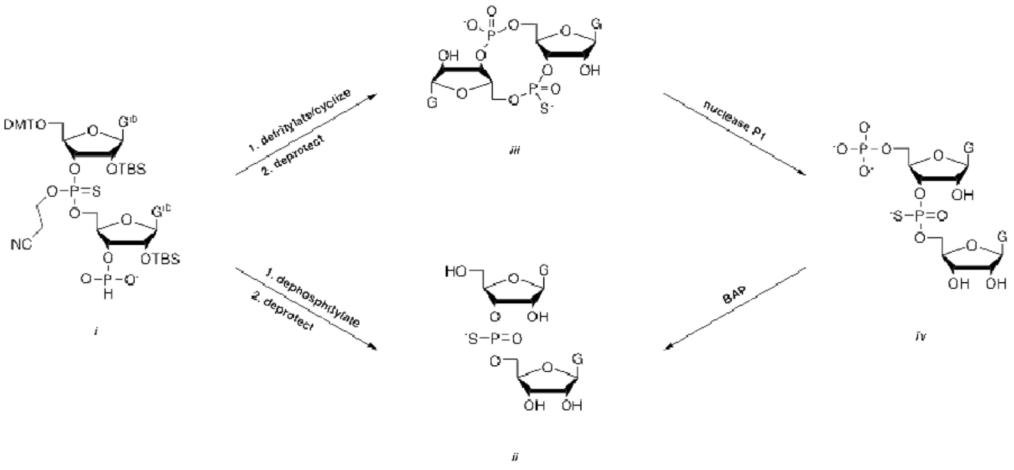

Scheme 2.

Table 1

Retention Times on RP HPLC (min) and ^{31}P NMR Chemical Shifts (ppm) at 55 °C for Dilute (0.5 mM) Samples of the Na^+ Salts of **5**–**7**

	RT	^{31}P δ
[R_P] Monothioate **5a**	6.1	−0.5, 55.4
[S_P] Monothioate **5b**	4.8	−0.3, 56.7
[R_P,R_P] Dithioate **6a**	8.0	55.4
[S_P,R_P] Dithioate **6b**	6.2	55.9, 57.4
[S_P,S_P] Dithioate **6c**	5.4	57.2
[R_P] Trithioate **7a**	9.1	55.3, 114.1
[S_P] Trithioate **7b**	8.0	57.2, 114.4

Table 2

Distribution of Complexes at 30 °C Based on Integration of ^{31}P NMR Spectra

		K^+ salts			Na^+ salts	
	# [S_P] sulfurs[a]	**%B[b]**	**% *anti* T/O[c]**	**% *syn* T/O[c]**	**%B[b]**	**% *anti* T/O[c]**	**% *syn* T/O[c]**
[R_P] Monothioate **5a**	0	5	60 O	35 O	50	33 T	17 T
[S_P] Monothioate **5b**	1	2	56 O	42 O	12	88 T	*e*
[R_P,R_P] Dithioate **6a**	0	7	60 O	33 O	49	35 T	16 T
[S_P,R_P] Dithioate **6b**	1	4	76 O	20 O	22	78 T	*e*
[S_P,S_P] Dithioate **6c**	2		*d*			*d*	
[R_P] Trithioate **7a**	1	5	64 O	31 O	26	74 T	*e*
[S_P] Trithioate **7b**	2		*d*			*d*	

[a] number of sulfurs in the [S_P] configuration,

[b] B=Bimolecular structure

[c] T/O=Tetra/Octamolecular complexes,

[d] =not determined due to extensive aggregation,

[e] no *syn* form was detectable